A neural population model of the bi-phasic EEG-power spectrum during general anaesthesia

Axel Hutt

A neural population model of the bi-phasic EEG-power spectrum during general anaesthesia

A. Hutt

1 Introduction

The neuronal mechanisms of general anaesthesia are still poorly understood though the induction of analgesia, amnesia, immobility and loss of consciousness by anaesthetic agents is well-established in hospital practice. To shed some light onto these mysterious effects, the last decades have focussed mainly onto the study of molecular effects of agents and their relation to anaesthetic end points. Then, a decade ago Steyn-Ross et al. were one of the first who studied the anaesthetic effects by a mathematical model of a neural population[1]. This model assumed a single neural population, i.e. a single brain area, that might experience external stochastic stimuli, e.g. from other populations. Although this model could not reproduce experimental data in all details, it gave a rather simple answer to the question of the origin of the loss of consciousness (LOC) during anaesthesia.

The success of this first model triggered the development of other mathematical models that consider different features of neural populations than the ones in the model of Steyn-Ross et al. and hence allow other answers to the question of LOC. The present work introduces a new rather simple model of neural population activity that shares properties with previous models and introduces others, see the following sections for more details. By virtue of its mathematical simplicity, it is the hope that it might serve as a basic model for general anaesthesia that may be extended easily by further neural functions while retaining its simple structure.

In hospital practice, typically a perioperative information management system is set up, e.g. to store medical records of patients and to manage different medical treatments during the patients stay (see Longnecker et al (2008), chapter 28). The system stores the physiological records extracted from monitoring systems that

A. Hutt
INRIA Grand Est - Nancy, Team CORTEX, 615 rue du Jardin Botanique, 54602 Villeres-les-Nancy, France e-mail: axel.hutt@inria.fr

[1] cf. Chapter 8 of Steyn-Ross et al. in this book.

measure certain medical variables. The origin of the word *monitor* is the Latin word *monere* that means *to warn*. Indeed, one of the important roles of monitoring is to alert the anaesthesist of changes in the patients' conditions. In addition, the monitoring system allows to use the information received to modify therapeutic interventions and hence to regulate and control the medical treatment of the patient. Such information may come from hemodynamic monitoring which measures e.g. arterial blood pressure, respiratory monitoring or intraoperative neurologic monitoring. The latter monitor detects electric activity on the scalp, the so-called electroencephalogram (EEG), that allows to reveal information on neural activity. The present work focusses on some anaesthetic-induced effects on the EEG.

The medical EEG may be classified into two subtypes, cf. chapter 32 in (Longnecker et al, 2008). Desynchronous EEG exhibits rather large frequencies with low amplitudes, which result from small groups of mutually active neurons. This EEG pattern is contrasted by synchronous EEG showing low frequencies with large amplitudes which are assumed to result from large populations of cortical neurons that are triggered by thalamic stimulation (Amzica and Steriade, 1998). The desynchronous EEG occurs when the subject is awake or during Rapid Eye Movement (REM)-sleep, while the synchronous EEG is observed during non-REM sleep, cerebral ischemia, sedation or anaesthesia. To detect the loss of consciousness in patients, the anaesthesist is interested in the change from desynchronous to synchronous EEG. To this end, typically the bispectral index BIS is computed indicating the depth of anaesthesia (Rampil, 1998). The decision at which index value the subject is unconscious is based on experience but the index range is limited. Typical BIS-values of the points of loss of consciousness are between 40 and 60 while BIS=100 and BIS$\ll 40$ mean fully awake and deep anaesthesia, respectively.

Increasing the administered dose of anaesthetic agent increases its blood plasma concentration and the EEG changes from desynchronous to synchronous EEG and the corresponding power spectrum may exhibit a bi-phasic behavior: at low agent concentration the power in certain frequency bands increase and finally decreases again for larger agent concentrations. This bi-phasic behavior can be found in the $\delta-$, $\theta-$, $\alpha-$ and $\beta-$ frequency band and the BIS is based on the power relation between these frequency bands. Since the BIS indicates well the loss of consciousness, the bi-phasic power spectrum is supposed to play an important role for the understanding of neural activity during anaesthesia.

To better understand the neural origin of the bi-phasic behavior of EEG, theoretical models have been developed. Such models describe mathematically the activity of a single neural population, cf. the chapters of Steyn-Ross et al., Liley et al. and Molaee-Ardekani et al. in this book. In brief, the original model approach of Steyn-Ross et al (2004) proposes the change of activity resting states as the deciding mechansim during the loss of consciousness and explains the bi-phasic behavior by this state change. The original models of Liley and Bojak (2005) and Molaee-Ardekani et al (2007) describe mathematically the bi-phasic behavior without a state change, but do not explain the loss of consciousness.

The model presented in this chapter differs mathematically from the previous ones and explains the bi-phasic behavior without a state change, but takes into ac-

count the possible state change. To illustrate this result, the subsequent section introduces the neural activity model and explains its difference to previous models in some detail. Then the synaptic effect of the anaesthetic agent propofol and its implementation into the model is discussed in subsection 2.2, followed by a brief analytical study of the number of resting states. Finally the last paragraphs in this section outlines the derivation of the systems' power spectrum and discusses the bi-phasic behavior found in the model activity. The last section summarizes the achieved results.

2 A neural population model

The present work considers an ensemble of neurons on a mesoscopic spatial scale in the range of cortical macrocolumns, i.e. on a spatial scale of some millimeters. It considers pyramidal cells and interneurons, and consequently involves excitatory and inhibitory synapses. Both types of synapses may occur on dendritic branches of both cell types. In the following, we consider excitatory synapses (abbreviated by e) at excitatory (E) and inhibitory cells (I) and take into account inhibitory synapses (i) at both cell types.

Moreover, by virtue of the large number of neurons in the ensemble the activity of synapses and neurons are treated as averages over the population in small spatial patches and short time windows, see e.g. (Hutt and Atay, 2005; Gerstner and Kistler, 2002). The mean postsynaptic potentials (PSP) at excitatory cells in a spatial patch at spatial location x and at time t is denoted $V_{E,s}(x,t)$ and originates from excitatory ($s = e$) or inhibitory ($s = i$) synapses which receive spiking activity from other pre-synaptic neurons. Similarly, the PSPs $V_{I,s}(x,t)$ are evoked at inhibitory cells by pre-synaptic activity at excitatory ($s = e$) or inhibitory ($s = i$) synapses.

The four PSPs are modelled by

$$\begin{aligned} V_{N,e}(x,t) - V_N^r &= \int_{-\infty}^{t} h_e(t-t') P_E(x,t')\, dt' \\ V_{N,i}(x,t) - V_N^r &= \int_{-\infty}^{t} h_i(t-t') P_I(x,t')\, dt' \end{aligned} \tag{1}$$

with $N = E$ for excitatory cells and $N = I$ for inhibitory cells, V_N^r is the resting potential of neurons of type N and P_E and P_I denote the pre-synaptic mean pulse activity originating from excitatory and inhibitory cells, respectively. Here we assume that axonal connections from excitatory cells terminate at excitatory synapses only, which holds true for over 80 percent of excitatory cells (Nunez, 1995). Further $h_e(t)$ and $h_i(t)$ represent the mean synaptic response functions of excitatory and inhibitory synapses and read (Koch, 1999)

$$h_e(t) = a_e \frac{\alpha_1\alpha_2}{\alpha_2-\alpha_1}\left(e^{-\alpha_1 t} - e^{-\alpha_2 t}\right) \tag{2}$$

$$h_i(t) = a_i f(p) \frac{\beta_1(p)\beta_2}{\beta_2-\beta_1(p)}\left(e^{-\beta_1(p) t} - e^{-\beta_2 t}\right). \tag{3}$$

with the temporal rates of the excitatory and inhibitory synapses $\alpha_{1,2}$ and $\beta_{1,2}$, respectively. This formulation of the mean synaptic response involves the various time scales of the synaptic response to an incoming spike, such as the membrane time constant of the dendrite, the voltage-dependent conductance change of the membrane (see e.g. Koch (1999), p.18) and the propagation delays along the dendritic tree (see e.g. Koch (1999), pp. 49). The parameter $p \geq 1$ in Eq. (3) denotes a weighting factor which reflects the propofol concentration and $f(p)$ quantifies the propofol action on the inhibtiory synapses. This formulation considers the synaptic effects of propofol only. In addition, a_e and a_i denote the level of excitation and inhibition, respectively.

Equations (1) give the mean synaptic responses in the ensemble and thus represent averages over all microscopic details of the synapto-dendritic system in the ensemble. Hence, the model does not take into account explicitely microscopic properties of synapses but consider their effect in the population.

For convenience, we may re-scale the time by $t \to \sqrt{\alpha_1\alpha_2}\,t$ and Eqs. (1) are rewritten as (Hutt and Longtin, 2009)

$$\hat{L}_e\left(V_{N,e}(x,t) - V_N^r\right) = a_e P_E(x,t) \tag{4}$$

$$\hat{L}_i(p)\left(V_{N,i}(x,t) - V_N^r\right) = a_i f(p)\,\omega_0^2(p) P_I(x,t)\,. \tag{5}$$

with the temporal operator $\hat{L}_s = \partial^2/\partial t^2 + \gamma_s \partial/\partial t + \omega_s^2, \quad s = e,i$ and

$$\begin{aligned} \omega_e^2 = 1 \quad &, \quad \omega_i = \omega_0^2(p) = \beta_1(p)\beta_2/\alpha_1\alpha_2 \\ \gamma_e = \sqrt{\alpha_1/\alpha_2} + \sqrt{\alpha_2/\alpha_1} \quad &, \quad \gamma_i = (\beta_1(p)+\beta_2)/\sqrt{\alpha_1\alpha_2}\,. \end{aligned}$$

To model the pre-synaptic mean pulse activity $P_E(x,t), P_I(x,t)$ at spatial location x subjected to the firing activity of other neurons at spatial location y, we assume spatially homogeneous synaptic interactions via axonal branches with

$$\begin{aligned} P_N(x,t) &= K_N * S_N[V - \Theta_N] \\ &= \int_\Omega K_N(x-y) S_N\left[V\left(y, t - \frac{|x-y|}{v}\right) - \Theta_N\right] dy. \end{aligned}$$

This ansatz considers a one-dimensional neural population embedded in the spatial domain Ω with periodic boundary conditions. Moreover v denotes the finite conduction speed of axonal connections. The functionals $S_E[\cdot]$, $S_I[\cdot]$ represent the somatic firing function of excitatory and inhibitory cells which have a sigmoidal shape (Freeman, 1979). The firing rate functions S_E, S_I are chosen to

$S_N(V) = S_m/(1+\exp(-c_N(V-\Theta_N)))$ and depend on the difference of the PSPs $V_{E,e} - V_{E,i}$ and $V_{I,e} - V_{I,i}$, respectively, since the corresponding synaptically evoked post-synaptic currents sum up at the neuron somata, cf. (Freeman, 1992; Hutt and Longtin, 2009). Moreover $\Theta_E,\ \Theta_I$ denote the corresponding mean firing thresholds. The synapses respond to cells which are located at different spatial locations and the functions $K_E,\ K_I$ account for the corresponding spatial nonlocal connectivity. They represent the probability density of connections from excitatory and inhibitory cells to excitatory and inhibitory synapses, respectively. This definition requires the normalisation to unity, i.e. $\int_\Omega K_{E,I}(x)dx = 1$. Then Eqs. (4), (5) read (Hutt and Longtin, 2009)

$$\begin{aligned} \hat{L}_e\left(V_e(x,t) - V_E^r\right) &= a_e K_E * S_E\left[V_e(x,t) - V_i(x,t) - \Theta_E\right] \\ \hat{L}_i(p)\left(V_i(x,t) - V_E^r\right) &= a_i f(p)\,\omega_0^2(p) K_I * S_I\left[V_e(x,t) - V_i(x,t) - \Theta_I\right] \end{aligned} \tag{6}$$

with the excitatory and inhibitory PSPs now defined as $V_e = V_{E,e}$ and $V_i = V_{E,i}$. Eqs. (6) are the final evolution equations of the neural activity, while the action of propofol is considered in $\hat{L}_i(p),\ f(p)$ and $\omega_0^2(p)$.

2.1 Yet another model ?

The neural field model (6) defines some basic elements of neural interactions in populations to describe the spectral properties in general anaesthesia. Other population models consider different neural interactions. Several of these models are based on the model of Liley et al (1999), see also the corresponding chapter in this book. This model considers a continuous spatial mean-field of neurons in one or two spatial dimensions, synapses and axonal connections and where the synapses and neurons may be excitatory and inhibitory. This mean-field represents the spatial average in a neural population description similar to the present work and thus averages the spiking activity of single neurons using a sigmoidal population firing rate. The firing activity is assumed to spread diffusively via a damped activity wave along the axonal trees and terminates at pre-synaptic terminals. The wave speed of this axonal wave is set to the mean axonal conduction speed and hence assumes a volume conduction mechanisms for the spread along axonal fibers. At the synaptic terminals the incoming pre-synaptic activity evokes the temporal synaptic response on the dendritic trees according to the dynamics of a single synapse, i.e. treating the membrane as an RC-circuit with a time-dependent conductance, see e.g. (Koch, 1999). Consequently the model neglects the spatial extension of dendritic trees due to this explicit model of single synapse responses.

The model considered in the present work is similar to the model of Liley et al. in several aspects but differs in some other important elements. In contrast to the Liley-model the presented model considers a population of synapses on den-

dritic trees (Koch, 1999) and the passive activity spread on dendrites (Agmon-Sir and Segev, 1993). To cope with the various delay distributions caused by the spatial distribution of synapses on the dendritic branches, the present model considers an average synaptic population response which obeys an average synaptic response function. In addition the present work models the activity transmission along axonal trees by taking into account the spatial probability density of axonal connections. This contrasts to the Liley-model, that assumes a volume conduction mechanism for the activity spread along the axonal branch. Interestingly, previous theoretical studies have shown that the mathematical treatment of connection probability densities extends the damped activity wave considered in the model of Liley et al. to nonlocal interactions, cf. (Coombes et al, 2007; Hutt, 2007).

Previous studies have explained the bi-phasic behavior in the EEG power spectrum by different mechanisms. Steyn-Ross et al (2004) support the idea that the bi-phasic spectrum and the LOC result from a first-order phase transition in the population. This phase transition reflects a sudden disappearance of the system's resting state accompanied by a jump to another resting state. The associated jump in state activity has been interpreted as the sudden loss of consciousness as observed in experiments, see the corresponding chapter in this book. In contrast, Bojak and Liley (2005) showed in an extensive numerical study of a slightly different model that such a phase transition is not necessary to reproduce bi-phasic power changes, but did not suggest a mechanism for the occurrence of LOC. Moreover Molaee-Ardekani et al (2007) introduced the idea of slow adaptive firing rates which explains the bi-phasic spectrum and LOC without a phase transition, see the corresponding chapter in this book. The present model aims to show that the bi-phasic power spectrum is not restricted to a spcific mechanism but may occur in the presence of both a single state, multiple states without an additional adaptive firing.

Summarizing, the model presented here simplifies specific aspects of the dynamics in single neurons but takes into account the major features. These features are the nonlinear gain of cells originating from the distribution of the neurons firing threshold, the synaptic response function covering the diverse properties of synapses and dendritic compartements, and the spatial and temporal aspects of axonal branches. By virtue of these simplifications, the model is mathematically less complex than the Liley-model since it has less parameters. This aspect allows for an analytical treatment of the model and, consequently, the analytical derivation of conditions for physiological parameters. The work aims to show that these elements are sufficient to describe the macroscopic dynamics of the neural population. This idea is supported by the marvellous work of Roxin et al (2006), who showed that neural field models may capture the macroscopic activity of a population of spiking neurons.

2.2 Synaptic anaesthetic effect

Our work focusses on the action of the anaesthetic agent propofol, which is a widely-applied anesthetic drug (Marik, 2004). It affects the cognitive abilities of subjects,

such as the response to auditory stimuli (Kuizenga et al, 2001) or pain (Andrews et al, 1997) and acts mainly on $GABA_A$ receptors, i.e. changes the response of inhibitory synapses. In detail, increasing the blood concentration of propofol yields an increase of the charge transfer in synaptic $GABA_A$-receptors and increases the decay time constant of their synaptic response function (Kitamura et al, 2002).

The current model approach describes mathematically the effect of varying properties of inhibitory synapses on the spatio-temporal dynamics of the neural ensembles, while the origin of such variations are the anaesthetic actions of propofol. Specifically, increasing the concentration of propofol prolongs the temporal decay phase of inhibitory $GABA_A$ synapses and increases the charge transfer in these synapse. In addition, the height of the synaptic response function is maintained for different propofol concentrations (Kitamura et al, 2002) in a good approximation.

To implement a similar behavior in our model, the factor p introduced in Eq. (3) reflects the target concentration of propofol in the neural population with $p = 1$ for vanishing propofol concentration. Since the function $f(p)$ introduced in Eq. (3) is set to affect the charge transfer in the inhibitory synapses, we choose the inhibitory charge transfer at vanishing propofol concentration such that $f(p = 1) = 1$, and identify the mean charge transfer with the level of the synaptic excitation or inhibition, cf. (Hutt and Longtin, 2009). Moreover, the model assumes that increasing p reflects an increasing propofol concentration which decreases the inhibitory decay rate by $\beta_1(p) = \beta_1^0/p$ with β_1^0 denoting the inhibitory decay rate in the absence of propofol. Consequently, $p = (1/\beta_1)/(1/\beta_1^0)$ represents the percentile increase of the inhibitory decay time constant. To mimic these assumption mathematically, we implement

$$f(p) = r^{-r/(r-1)}\,(rp)^{rp/(rp-1)}\ ,\ r = \beta_2/\beta_1 \tag{7}$$

which guarantees a constant height of the impulse response function $h_i(t)$ and reflects an increasing charge transfer of the inhibitory synapse $f(p)$ with increasing p. Typically the decay phase of the synaptic response curve is much longer than its rise phase, i.e. $\beta_1 \ll \beta_2,\ r \gg 1$ and thus $f(p) \approx p$.

To investigate the validity of the model assumptions, we consider experimental results on the synaptic response of $GABA_A$-synapses measured *in-vitro* in cultured cortical neurons of rats (Kitamura et al, 2002). Figure 1(a) shows the mean values p obtained experimentally at $GABA_A$-synapses subject to the propofol concentration c, together with the extreme values of p at the borders of the error bars. The dependence of the percentile increase of the decay time constant p on the concentration c is set to $p(c) = k_1 * ln(k_2 + k_3 * c)$ and the constants $k_1,\ k_2,\ k_3$ are mean-least square fitted to the experimental data. In addition Fig.1(b) gives the corresponding mean and extreme values of the normalized charge transfer $ct(c)$ obtained experimentally. This function is mean least-square fitted to $ct(c) = k_4 * ln(k_5 + k_6 * c)$ with the constants $k_4,\ k_5,\ k_6$. Then the normalized charge transfer subjected to the factor p can be computed to $ct(p) = f(p) = b_0 \ln(b_1 + b_2 e^{b_3 p})$ with $b_0 = k_4,\ b_1 = k_5 - k_2 k_6/k_3,\ b_2 = k_6/k_3,\ b_3 = 1/k_1$. Figure 1(c) shows $ct(p)$, the corresponding

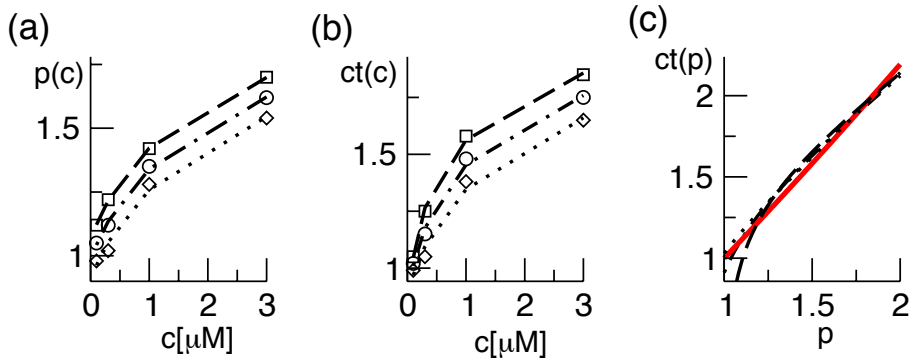

Fig. 1 Extraction of the charge transfer curve from experimental data (Fig. 6 in (Kitamura et al, 2002)) subjected to the factor p. The panel (a) shows the experimentally measured mean (circles) percental increase of the inhibitory decay time p, their maximum (squares) and minimum (diamonds) values at the error interval borders and the corresponding fitted functions $p(c)$ (dashed line for maximum values, dashed-dotted line for the mean value and dotted line for the minimum values). (b) shows the experimentally measured mean (circles) percental increase of the charge transfer, their maximum (squares) and minimum (diamonds) values at the error interval borders and the corresponding functions $ct(c)$, the line coding is the same as in (a). (c) presents the calculated relation $ct(p)$ for the mean values, the lower and upper value border and the model (red solid line), see text for model details. The line coding is the same as in (a).

functions obtained from the error borders and the model function (7) with $r = 8.5$ and we observe good accordance. Consequently the charge transfer model (7) is reasonable for $\beta_2 \approx 8.5\beta_1$.

Since the study on propofol effects in (Kitamura et al, 2002) are based on experiments on rats, it is interesting to link the results to humans. In human general anaesthesia, the value EC_{50} gives the concentration of the anesthetic agent for which 50 of 100 subjects are anesthesized, i.e. do not respond to external stimuli or surgical incision. For the administration of propofol, a typical concentration is $0.2\mu\mathrm{M}/\mathrm{ml}$ ($\sim 2\mu\mathrm{g}/\mathrm{ml}$) (Franks and Lieb, 1994), which corresponds to $p \approx 1.2$, cf. Fig. 1. For unit conversion of the propofol concentrations, the rule $1\mu\mathrm{g} \approx 0.1\mu\mathrm{M}$ holds (Franks and Lieb, 1994).

Summarizing, increasing the factor p prolongs the decay phase and increases the charge transfer in inhibitory synapses while maintaining the amplitude of the resulting IPSPs constant. Figure 2 shows the simulated temporal impulse response of an inhibitory $GABA_A$ synapse h_i as a function of time and the factor p. We observe a constant amplitude and a prolonged decay phase for increasing p, as desired.

2.3 Multiple resting states

To gain insight into the resting activity of the neural population, first let us investigate the stationary solutions $\bar{V}_e$, $\bar{V}_i$ of Eqs. (6), which are assumed constant in space

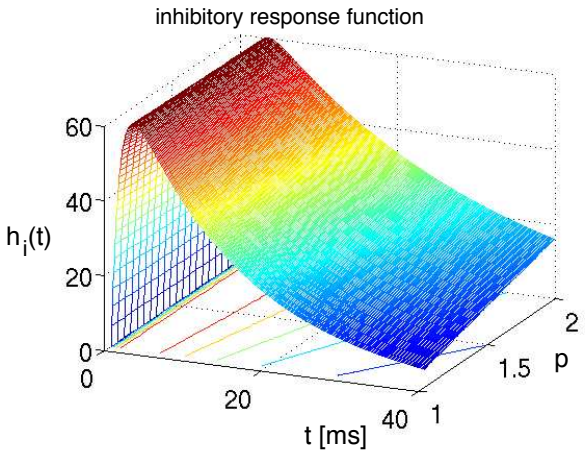

Fig. 2 The temporal impulse response function $h_i(t)$ of inhibitory synapses subject to various values of p taken from (3) and (7). Parameters are set to $\beta_1^0 = 75$Hz, $\beta_2 = 1000$Hz, which are typical for $GABA_A$-synapses (Koch, 1999).

and time. Introducing the new variables $\bar{V}_- = \bar{V}_e - \bar{V}_i$ and $\bar{V}_+ = \bar{V}_e + \bar{V}_i$, Eqs. (6) decouple to

$$\bar{V}_- = a_e S_E\left[\bar{V}_- - \Theta_E\right] - f(p) a_i S_I\left[\bar{V}_- - \Theta_I\right] \tag{8}$$

$$\bar{V}_+ = a_e S_E\left[\bar{V}_- - \Theta_E\right] + f(p) a_i S_I\left[\bar{V}_- - \Theta_I\right] + 2V_E^r\,. \tag{9}$$

Here $\bar{V}_-$ is the stationary mean membrane potential which triggers the spike generation in the neural population at the global resting state. Equations (8), (9) reveal that it is sufficient to determine $\bar{V}_-$ from Eq. (8) to find $\bar{V}_-$ and $\bar{V}_+$ and hence the number of solutions $\bar{V}_-$ gives the number of stationary solutions.

A detailed study of the number of roots (Hutt and Longtin, 2009) yields conditions for (a) three resting states for a limited range of values of p and a single resting state otherwise and (b) a single stationary state for all p. The three stationary solutions have been studied previously in some analytical details by Steyn-Ross et al (2001) and the single stationary solution has been considered numerically by Bojak and Liley (2005); Molaee-Ardekani et al (2007). These studies are based on the Liley-model. In the following, we refer to the case of the single stationary solution as the single solution case and to the case of three stationary solutions as the triple solution case.

Figure 3 shows the solutions $\bar{V}_-$, and the resulting firing rates of excitatory and inhibitiory neurons $S_E(\bar{V}_- - \Theta_E)$ and $S_I(\bar{V}_- - \Theta_I)$, resp., with respect to the weight factor p. In the triple solution case (Fig. 3(a)), the system starts at a high firing rate

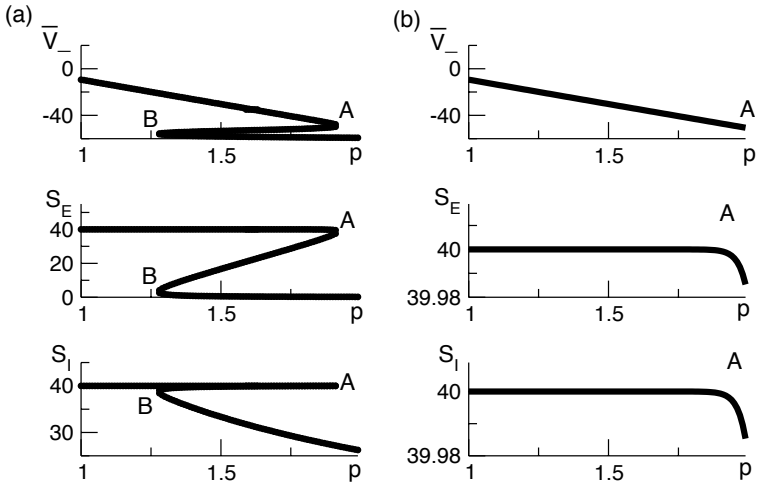

Fig. 3 The stationary solutions $\bar{V}_-$ of Eq. (8), the firing rates of excitatory and inhibitory neurons $S_E = S_E(V-\Theta_E)$ and $S_I = S_I(V-\Theta_I)$, respectively,for both solution cases. (a) $\Theta_E > \Theta_I$, $c_e = c_i$, (b) $\Theta_E = \Theta_I$, $c_e = c_i$. The specific parameters are (a) $\Theta_E = -53$mV, $\Theta_I = -60$mV, $c_e = c_i = 0.84/$mV, (b) $\Theta_E = \Theta_I = -60$mV, $c_e = c_i = 0.24/$mV. Additional parameters are $a_e = 1$mV/s, (a) $a_i = 0.2$mV/s, (b) $a_i = 1.4$mV/s.

at $p = 1$ and shows an activity decrease up to point A. Then a further increase of p causes the stationary excitatory firing activity to discontinuously jump to smaller values. In addition we observe a top, center and bottom solution branch. Likewise, the single stationary solution (Fig. 3(b)) exhibits a decrease of the firing rate while increasing p. However, here the drop of activity is continuous and the firing rate changes less aprupt than in the triple solution case. Such a continuous decrease of the firing rate while increasing the propofol concentration has been reported experimentally in cultures of rat neocortical tissue (Antkowiak, 1999).

In mathematical terms, the triple solution case exhibits a saddle-node bifurcation and the first discontinuous drop of activity at point A. This bifurcation occurs if the left and right hand side of Eq. (8) exhibit the same derivative with respect to $\bar{V}_-$, i.e.

$$1 = a_e \delta_E(p) - a_i f(p) \delta_I(p) \; . \tag{10}$$

Here $\delta_E(p) = \partial S_E[V(p)-\Theta_E]/\partial V$, $\delta_I(p) = \partial S[V(p)-\Theta_I]/\partial V$ evaluated at $V = \bar{V}_-$ represent the so-called non-linear gains of the system. Since $\delta_E(p)$, $\delta_I(p)$ are the slopes of the transfer functions S_E, S_I, they reflect the conversion of membrane potentials to the spike firing activity. In contrast to the triple solution case, the single stationary solution does not show this activity drop and exhibits $1 > a_e \delta_E(p) - a_i f(p) \delta_I(p)$ for all values of p, i.e. condition (10) never holds.

2.4 The biphasic power spectrum

A prominent measure to determine the depth of general anaesthesia is the power spectrum of the subject's electroencephalogram (EEG). As outlined in section 1, the prominent effect in power spectra during general anaesthesia is the biphasic change of frequency power while increasing the propofol concentration, i.e. the increase and then decrease of spectral power in the $\delta-$, $\theta-$, $\alpha-$ and $\beta-$ band. To model this change of the power spectrum with respect to the factor p, the subsequent paragraphs derive the power spectrum of the EEG. The derivation of the power spectrum follows previous studies on the effect of finite axonal conduction speed on the activity of neural populations involving a single neuron type (Hutt and Atay, 2007; Hutt and Frank, 2005).

The power spectrum

The power spectrum represents a statistical measure of the system's linear response to a spatio-temporal external input. This input might originate from other neural populations and is assumed small compared to the resting states $\bar{V}_e$, $\bar{V}_i$ defined by Eqs. (8), (9). Moreover the power spectrum is defined in the linear regime and the system remains close to the resting state if it is linearly stable, see Hutt and Longtin (2009) for a detailed study of the systems' stability. In the following, we assume that the system is stable, i.e. small perturbations do not repel the system too far from its stationary state determined in section 2.3.

Considering the excitatory external input $\Gamma(x,t)$, the identities $\hat{L}_{e,i}h_{e,i}(t) = \delta(t)$ and linear terms only, Eqs. (6) read

$$u_e(x,t) = a_e\delta_E \int_{-\infty}^{t} d\tau h_e(t-\tau) \times \int_\Omega dy K_e(x-y)\left(u_e(y,\tau-\frac{|x-y|}{v}) - u_i(y,\tau-\frac{|x-y|}{v})\right) + \Gamma(x,t) \tag{11}$$

$$u_i(x,t) = a_i\delta_I f\omega_0^2 \int_{-\infty}^{t} d\tau h_i(t-\tau) \times \int_\Omega dy K_i(x-y)\left(u_e(y,\tau-\frac{|x-y|}{v}) - u_i(y,\tau-\frac{|x-y|}{v})\right) \tag{12}$$

The variables $u_e(x,t) = V_e(x,t) - \bar{V}_e$ and $u_i(x,t) = V_i(x,t) - \bar{V}_i$ denote the deviations from the stationary states $\bar{V}_e$ and $\bar{V}_i$ and depend linearly on the evoked currents in the membrane, that are present in the dendritic tree and its surrounding. These evoked currents propagate along the dendritic branch towards and away from the trigger zone at the neuron soma. Since excitatory and inhibitory currents add up at the trigger zone and have different signs, the corresponding potentials also sum up at the trigger zone. This means the effective membrane potential $u_e(x,t) - u_i(x,t)$ is

proportional to the current that flows in the tissue close to the dendritic branch and along the dendritic branch. This physical effect is supposed to represent the origin of the EEG since the evoked current represents a current dipole that generates the electromagnetic activity on the scalp. Such currents are measured experimentally by electrodes in the neural tissue and the corresponding potentials are the LFPs. Consequently LFPs reflect the dendritic currents or correspondingly the membrane potentials on the dendrites. Since the EEG represents the spatial average of the dendritic activity in a good approximation, cf. the book of Nunez and Srinivasan (2006), we consider the effective membrane potential $u(x,t) = u_e(x,t) - u_i(x,t)$ which is proportional to the dendritic currents.

The neural population activity is assumed to be in a stationary state in the presence of the external stationary input. Then the ergodicity assumption holds and the power spectrum of $u(x,t)$ at the spatial location x is given by the relation

$$P_{LFP}(x,\omega) = \frac{1}{\sqrt{2\pi}} \int_{-\infty}^{\infty} d\tau \, C_{LFP}(x,\tau) e^{i\omega\tau} \tag{13}$$

with the autocorrelation function $C_{LFP}(x,\tau) = \langle u(x,t)u(x,t-\tau)\rangle$ and the ensemble average $\langle \cdots \rangle$, i.e. the average over many realizations.

The external input to the network $\Gamma(x,t)$ represents the excitatory synaptic responses to random fluctuations uncorrelated in space and time $\xi(x,t)$ with $\langle \xi(x,t)\rangle = 0$, $\langle \xi(x,t)\xi(y,T)\rangle = Q\delta(x-y)\delta(t-T)$ and the fluctuation strength Q and the input reads

$$\Gamma(x,t) = \int_{-\infty}^{t} d\tau h_e(t-\tau)\xi(x,\tau) \tag{14}$$

with the synaptic response function $h_e(t)$ taken from Eq. (2). To obtain the autocorrelation function, we apply linear response theory (Hutt and Longtin, 2009) and find

$$C_{LFP}(x,\tau) = \frac{Q}{(2\pi)^3} \int_{-\infty}^{\infty} dk \int_{-\infty}^{\infty} d\omega \, |\tilde{G}(k,\omega)|^2 |\bar{h}_e(\omega)|^2 e^{-i\omega\tau} \, . \tag{15}$$

Here

$$\tilde{G}(k,\omega) = \frac{1}{\sqrt{2\pi}} \left(1 - \sum_{n=0}^{\infty} \mathscr{L}_n(k,\omega) \, (-i\omega)^n \right)^{-1}$$

is the Fourier transform of the Greens function with

$$\begin{aligned}
\mathscr{L}_n(k,\omega) &= \frac{1}{n!} \left(-\frac{1}{v} \right)^n \int_0^{\infty} dt \left(a_e \delta_E h_e(t) \tilde{K}_e^n(k) - a_i \delta_I f \omega_0^2 h_i(t) \tilde{K}_i^n(k) \right) e^{i\omega t}, \\
\tilde{K}^n(k) &= \int_{\Omega} dz K(z) |z|^n e^{-ikz}, \\
\bar{h}_e(\omega) &= \int_0^{\infty} dt h_e(t) e^{i\omega t} \, .
\end{aligned}$$

Then applying the Wiener-Khinchine theorem the power spectrum is computed to

$$P_{LFP}(x,\nu) = \frac{Q}{(2\pi)^{7/2}} \int_{-\infty}^{\infty} dk\, |\tilde{G}(k,\nu)|^2 |\bar{h}_e(\nu)|^2. \tag{16}$$

with the frequency $\nu = \omega/2\pi$. Equations (15) and (16) reveal that the correlation function and the power spectrum are independent of the spatial location which reflects the spatial homogeneity of the population.

To obtain the power spectrum of the EEG, we take into account the large distance of the EEG-electrode from the neural sources and the spatial low-pass filtering of the scalp and bone (Srinivasan et al, 1998; Nunez and Srinivasan, 2006). Then as a first good approximation the EEG activity represents the spatial summation of electric activity $u_{EEG}(t) = \int_\Omega dx\, u(x,t)$. Here we assume that the EEG-electrodes are far from the neural population compared to the spatial extension of the population. This is reasonable since EEG is measured on the scalp, which typically has a distance of a few centimeters from neural areas with a diameter of a few millimeters.

Assuming the external input as the excitatory synaptic response to uncorrelated random fluctuations, we obtain finally

$$C_{EEG}(\tau) = Q(2\pi)^2 \int_{-\infty}^{\infty} d\omega\, |\tilde{G}(0,\omega)|^2 |\bar{h}_e(\omega)|^2 e^{-i\omega\tau}. \tag{17}$$

$$P_{EEG}(\nu) = \frac{Q}{\sqrt{2\pi}} |\tilde{G}(0,\nu)|^2 |\bar{h}_e(\nu)|^2 \tag{18}$$

with the fluctuation strength Q. Equation (18) represents the power spectrum of the EEG measured on the scalp and, hence, the quantity that is measured in general anaesthesia. The advantage of this detailed mathematical formulation is the possibility of an analytical study of the bi-phasic power spectrum behavior. This study has been performed in a recent work (Hutt and Longtin, 2009) and conditions for the occurence of the bi-phasic spectrum have been derived analytically.

The biphasic spectrum

At first we impose the condition that the power increases at low frequencies when increasing the propofol concentration, i.e. $dP_{EEG}(0)/dp > 0$. For the triple solution case, this condition yields

$$a_e/a_i > e^{-\bar{c}\eta} \left(\frac{1-\rho}{1-\rho e^{\bar{c}\eta}} \left(\frac{1+\rho e^{\bar{c}\eta}}{1+\rho} \right)^3 f + \frac{1-\delta_E a_e + \delta_I a_i f}{S_m \bar{c} a_i} \frac{(1+\rho e^{\bar{c}\eta})^3}{(1+\rho)(1-\rho e^{\bar{c}\eta})} \right) \tag{19}$$

with $\rho(p) = \exp(-\bar{c}(\bar{V}_- - \Theta_I))$ and $\eta = \Theta_E - \Theta_I > 0$. We find that the parameter regime of the power enhancement is large for shallow firing rate functions (Hutt and Longtin, 2009). Figure 4(a) shows the power spectrum enhancement for the triple

solution case and we observe a bi-phasic behavior in the spectrum.

To extend the imposed conditions on the power spectrum, the experimental findings also stipulate the decrease of power at large frequencies for large values of p. Hence the condition for a power increase at low frequencies and a power decrease at high frequencies read $dP_{EEG}(0)/dp > 0$ and $dP_{EEG}(\nu)/dp < 0, \nu \gg 0$, respectively. For a large but finite axonal conduction speed, we find the conditions (Hutt and Longtin, 2009)

$$\begin{aligned} dP_{EEG}(0)/dp > 0 \;\rightarrow\; a_e/a_i > \frac{\partial}{\partial p}(f(p)\delta_I(p))/\frac{\partial \delta_E(p)}{\partial p} \\ dP_{EEG}(\nu)/dp < 0 \;\rightarrow \frac{d\mathscr{L}_{0,r}}{dp}(1-\mathscr{L}_{0,r}) > 0 \end{aligned} \tag{20}$$

with

$$\begin{aligned} \mathscr{L}_{0,r} &= A_e(\nu)\delta_E(p) - A_i(p,\nu)\delta_I(p)f(p)\omega_0^2(p) \\ A_e(\nu) &= \frac{1-(2\pi\nu)^2}{1+(2\pi\nu)^2(\gamma_e^2-2)+(2\pi\nu)^4}\ , \\ A_i(p,\nu) &= \frac{\omega_0^2(p)-(2\pi\nu)^2}{\omega_0^4(p)+(2\pi\nu)^2(\gamma_i^2(p)-\omega_0^2(p))+(2\pi\nu)^4}\ . \end{aligned}$$

The conditions (20) define the parameter set for bi-phasic behavior. We focus on the single solution case and apply a numerical parameter search in $\bar{c}, a_i, \beta_1$ which satisfies conditions (20) considering the result $\beta_2 = 8.5\beta_1$ from section 2.2. Figure 4(b) presents the spectral power enhancement for a set of parameters obtained numerically. The power in the $\delta-$, θ- and $\alpha-$band exhibits a sequential increase and decrease of power in according to experiments. Moreover the maxima of the $\alpha-$ and $\delta-,\theta-$power occur at $p \approx 1.4$ and $p \approx 1.6$ and thus at concentrations 1μM ($\sim 0.5\mu$g) and 2μM ($\sim 1.1\mu$g), respectively. These concentrations are similar to medical effect-site concentrations during surgery and Fig. 4(b) shows good accordance to the biphasic behavior observed experimentally in general anaesthesia.

3 Summary

The presented work introduces a novel neural population model to describe mathematically the effect of the anaesthetic propofol on the EEG-power spectrum. The study shows a bi-phasic spectrum in the presence of both multiple states and a single state. On the one hand, it can be concluded, that multiple states are not necessary to gain a bi-phasic power spectrum. Since the loss of consciousness (LOC) during anaesthesia is related to the bi-phasic behavior, one may argue that LOC may occur in the presence of a single stable state. Consequently the jump between stable states

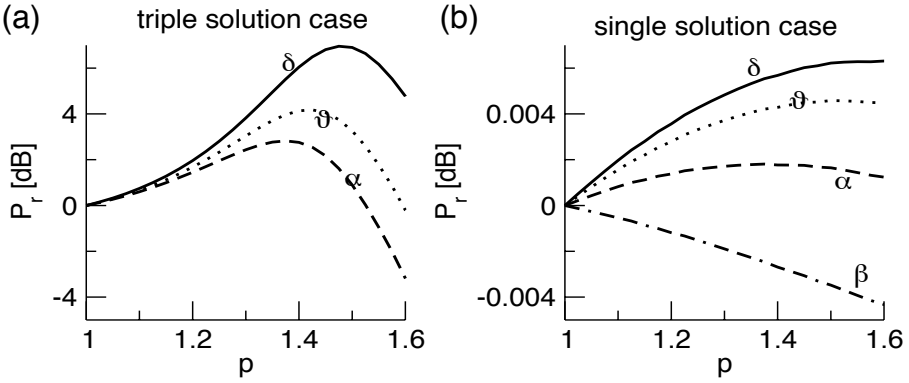

Fig. 4 Spectral power enhancement $P_e(p)$ for the triple (a) and single (b) solution case. Here it is $P_r(p) = 10\log_{10}(P_{EEG}(p)/P_{EEG}(p=1))$ in the corresponding frequency bands, and the frequency bands are defined in the intervals $[0.1\text{Hz};4\text{Hz}]$ (δ-band), $[4\text{Hz};8\text{Hz}]$ (θ-band), $[8\text{Hz};12\text{Hz}]$ (α-band) and $[12\text{Hz};20\text{Hz}]$ (β-band). Parameters are (a) $\Theta_E = -50\text{mV}, \Theta_I = -60\text{mV}$, $c_e = c_i = 0.114/\text{mV}$ and $a_i = 1.4\text{mVs}$ on the top branch, (b) $\Theta_E = \Theta_I = -60\text{mV}$, $c_e = c_i = 0.038/\text{mV}$ and $a_i = 0.2\text{mVs}$. Other parameters are $a_e = 1.0\text{mVs}$, $\beta_2 = 5780\text{Hz}$, $\beta_1 = 680\text{Hz}$, $\alpha_1 = 222\text{Hz}$, $\alpha_2 = 5000\text{Hz}$.

at the LOC as argued by Steyn-Ross et al. is not necessary to observe the LOC.
On the other hand, a very recent experimental study on insects and mammals of Friedman et al (1992) demonstrates that changing the anaesthetic concentration in neural tissue induces phase transitions with hysteresis. This transition is independent of the pharmaco-dynamics and -kinetics of the agent. Consequently increasing the anaesthetic agent concentration yields a drop of neural population activity from high activity to low activity, which may explain the loss of consciousness as a loss of neural activity. More future experimental and theoretical work on this topic will elucidate the details of the LOC.

References

Agmon-Sir H, Segev I (1993) Signal delay and input synchronisation in passive dendritic structures. J Neurophysiol 70:2066–2085

Amzica F, Steriade M (1998) Electrophysiological correlates of sleep delta waves. Electroencephalogr Clin Neurophysiol 107:69–83

Andrews D, Leslie K, Sessler D, Bjorksten A (1997) The arterial blood propofol concentration preventing movement in 50incision. Anesth Analg 85:414–419

Antkowiak B (1999) Different actions of general anesthetics on the firing patterns of neocortical neurons mediated by the GABAA-receptor. Anesthesiology 91:500–511

Bojak I, Liley D (2005) Modeling the effects of anesthesia on the electroencephalogram. Phys Rev E 71:041,902

Coombes S, Venkov N, Shiau L, Bojak I, Liley D, Laing C (2007) Modeling electrocortical activity through improved local approximations of integral neural field equations. PhysRevE 76:051,901–8

Franks N, Lieb W (1994) Molecular and cellular mechanisms of general anesthesia. Nature 367:607–614

Freeman W (1979) Nonlinear gain mediating cortical stimulus-response relations. Biol Cybern 33:237–247

Freeman W (1992) Tutorial on neurobiology: from single neurons to brain chaos. Int J Bif Chaos 2(3):451–482

Friedman EB, Sun Y, Moore JT, Hung HT, Meng QC, Perera P, Joiner WJ, Thomas SA, Eckenhoff RG, Sehgal A, Kelz MB (1992) A conserved behavvioral state barrier impedes transitions between anesthetic-induced unconsciousness and wakefulness: evidence for neural inertia. PLoS One 5(7):e11903

Gerstner W, Kistler W (2002) Spiking Neuron Models. Cambridge University Press, Cambridge

Hutt A (2007) Generalization of the reaction-diffusion, Swift-Hohenberg, and Kuramoto-Sivashinsky equations and effects of finite propagation speeds. Phys Rev E 75:026,214

Hutt A, Atay F (2005) Analysis of nonlocal neural fields for both general and gamma-distributed connectivities. Physica D 203:30–54

Hutt A, Atay F (2007) Spontaneous and evoked activity in extended neural populations with gamma-distributed spatial interactions and transmission delay. Chaos, Solitons and Fractals 32:547–560

Hutt A, Frank T (2005) Critical fluctuations and 1/f -activity of neural fields involving transmission delays. Acta Phys Pol A 108(6):1021

Hutt A, Longtin A (2009) Effects of the anesthetic agent propofol on neural populations. Cogn Neurodyn 4(1):37–59

Kitamura A, Marszalec W, Yeh J, Narahashi T (2002) Effects of halothane and propofol on excitatory and inhibitory synaptic transmission in rat cortical neurons. J Pharmacol 304(1):162–171

Koch C (1999) Biophysics of Computation. Oxford University Press, Oxford

Kuizenga K, Wierda J, Kalkman C (2001) Biphasic eeg changes in relation to loss of consciousness during induction with thiopental, propofol, etomidate, midazolam or sevoflurane. Brit J Anaesth 86(3):354–360

Liley D, Bojak I (2005) Understanding the transition to seizure by modeling the epileptiform activity of general anaesthetic agents. J Clin Neurophysiol 22:300–313

Liley D, Cadusch P, Wright J (1999) A continuum theory of electrocortical activity. Neurocomp 26-27:795–800

Longnecker DE, Brown DL, Newman MF, Zapol WM (eds) (2008) Anesthesiology. McGraw Hill, New York

Marik P (2004) Propofol: Therapeutic indications and side-effects. Curr Pharm Des 10(29):3639–3649

Molaee-Ardekani B, Senhadji L, Shamsollahi M, Vosoughi-Vahdat B, EWodey (2007) Brain activity modeling in general anesthesia: Enhancing local mean-field models using a slow adaptive firing rate. Phys Rev E 76:041,911

Nunez P (1995) Neocortical dynamics and human EEG rhythms. Oxford University Press, New York - Oxford

Nunez P, Srinivasan R (2006) Electric Fields of the Brain: The Neurophysics of EEG. Oxford University Press, New York - Oxford

Rampil I (1998) A primer for eeg signal processing in anaesthesia. Anesthesiol 89:980–1002

Roxin A, Brunel N, Hansel D (2006) Rate models with delays and the dynamics of large networks of spiking models. Prog Theor Phys 161:68–85

Srinivasan R, Nunez P, Silberstein R (1998) Spatial filtering and neocortical dynamics: estimates of eeg coherence. IEEE TransBiomed Eng 45:814–827

Steyn-Ross M, Steyn-Ross D, Sleigh J, Wilcocks L (2001) Toward a theory of the general-anesthetic-induced phase transition of the cerebral cortex: I. a thermodynamic analogy. Phys Rev E 64:011,917J

Steyn-Ross M, Steyn-Ross D, Sleigh J (2004) Modelling general anaesthesia as a first-order phase transition in the cortex. Prog Biophys Molecul Biol 85(2-3):369–385